The Astrophysical Journal, 613:L157–L160, 2004 October 1

ACCRETION EFFICIENCY DURING PLANETARY COLLISIONS

Craig Agnor and Erik Asphaug
Department of Earth Sciences, University of California at Santa Cruz, 1156 High Street, Santa Cruz, CA 95064; cagnor@es.ucsc.edu
Received 2004 March 29; accepted 2004 August 17; published 2004 August 31

ABSTRACT

We present the results of smoothed particle hydrodynamic simulations of collisions between two 0.10 $M_\oplus$ differentiated planetary embryos with impact dynamics that are thought to be common to the late stage of terrestrial planet formation. At low impact velocities ($v_{\rm imp}/v_{\rm esc} < 1.5$) and for direct collisions, the impacts are largely accretionary. Inelastic bouncing between embryos with varying degrees of erosion, followed by escape to infinity, is also a common outcome. For dynamical environments typical of most late-stage accretion models, we estimate that more than half of all collisions between like-sized planetary embryos do not result in accumulation into a larger embryo.

Subject headings: accretion, accretion disks — planets and satellites: formation — solar system: formation

1. INTRODUCTION

The standard model for the formation of the terrestrial planets describes their growth as the collisional accumulation of rocky planetesimals. This model is typically divided into three stages: (1) the formation of kilometer-sized planetesimals requiring 10^2–10^4 yr; (2) the runaway and oligarchic accumulation of planetesimals into $\sim 10^3$ km planetary embryos requiring 10^5–10^6 yr; and (3) the late stage, in which planetary embryos perturb each other into crossing orbits and suffer large impacts until the remaining planets become isolated and cease to encounter or collide with each other (see reviews by Wetherill 1990; Lissauer & Stewart 1993; Canup & Agnor 2000).

Studies of the accretion of planetary embryos (stage 2) generally indicate that their accumulation is rapid, requiring only $\sim 10^6$ yr to form 0.01–0.10 $M_\oplus$ objects, where $M_\oplus$ is an Earth mass (e.g., Wetherill & Stewart 1993). At this time, planetary embryos likely contain 50% (Kokubo & Ida 1998) to as much as 90% (Weidenschilling et al. 1997) of the total mass of the terrestrial system. During stage 3, collisions between large, like-sized embryos are common. They are of particular importance as they represent a principal evolutionary process, ultimately influencing many physical and chemical characteristics of the planets. For example, the collisional and encounter histories of planets may directly determine the mass, isotopic composition (e.g., Zhang 2002), extent of volatile depletion, rotation states (e.g., Lissauer et al. 2000), bulk composition (Benz et al. 1988), and formation of impact-generated satellites (e.g., Canup 2004). In addition, the generation of collisional fragments may alter accretion dynamics (i.e., orbital elements and encounter velocities may be damped via dynamical friction; e.g., Wetherill & Stewart 1993). Finally, collisions are counted on to explain diverse aspects of the meteoritic rock record (e.g., Keil 2000).

Despite the central role played by collisions in facilitating accretion, relatively little is known of collision outcomes between $R \sim 10^3$ km objects. Indeed, partially owing to the absence of a fragmentation model appropriate to this regime and to the N^2 computational cost (where N is the number of embryos tracked directly), most late-stage accretion models simply treat collisions as inelastic mergers. However, tracking the evolution of a growing planet's spin state using perfectly inelastic accretion leads to growing planets with rotation speeds greater than the orbital speed at the equator of a sphere of equivalent mass (see, e.g., Agnor et al. 1999, hereafter ACL99). This is a strong indication that the outcome of late-stage collisions is not well described by simple mergers.

Here we present the results of smoothed particle hydrodynamic (SPH) simulations of collisions between planetary embryos thought common during the late stage of terrestrial planet accretion. In our initial survey of late-stage collisions, we focus on the relatively simple issue of accretion efficiency and the morphology of collision outcomes. That is, to what extent is the material of two colliding bodies combined into a larger object? When is the use of inelastic mergers a good approximation of collision outcomes? What are the general collision morphologies that occur during planet formation?

2. BACKGROUND

2.1. *Impact Dynamics*

We parameterize collision dynamics by impact velocity ($v_{\rm imp}$) and impact angle (ξ). The impact velocity is a function of both the relative velocity at infinity (v_∞) and the two-body escape velocity ($v_{\rm esc}$) with $v_{\rm imp}^2 = v_{\rm esc}^2 + v_\infty^2$. For an encounter involving a target and impactor with masses (M_t, M_i) and radii (R_t, R_i), respectively, the two-body escape velocity is $v_{\rm esc}^2 = 2G(M_i + M_t)/(R_i + R_t)$. We use an impact angle (ξ) defined as the angle between the relative position and velocity vectors when the two bodies are in contact (i.e., $\xi = 0°$ for a head-on collision and $\xi = 90°$ for a grazing encounter). Assuming an isotropic flux of impactors, the probability of a collision with ξ in the range $\xi \rightarrow \xi + d\xi$ is $dP = 2 \sin \xi \cos \xi \, d\xi$ (Shoemaker 1962).

2.2. *Previous Impact Models*

To date, collision studies applicable to stage 3 have had two main emphases: (1) determining how well individual collisions explain particular planetary characteristics (e.g., the formation of the Moon) or (2) developing scaling relations for catastrophic disruption of the target (e.g., Holsapple et al. 2002). SPH modeling of the giant impact thought responsible for the origin of the Moon has generally considered collisions between a 0.5–0.9 $M_\oplus$ proto-Earth and a 0.1–0.3 $M_\oplus$ planetary embryo with $v_{\rm imp} = 1.0 v_{\rm esc}$–$1.2 v_{\rm esc}$ (see, e.g., Benz et al. 1989; Cameron 2001; Canup & Asphaug 2001; Canup 2004). These low-velocity collisions are highly accretionary, with most of the mass of the impactor ending up gravitationally bound to the target.

Studies of collisional disruption have focused on the higher

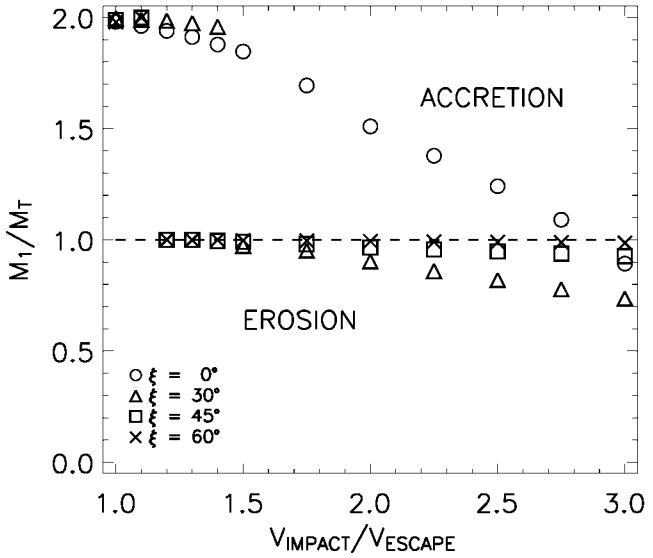

FIG. 1.—Mass of the largest gravitationally bound aggregate (M_1) scaled by the target mass (M_t) as a function of the impact velocity. The horizontal line indicates the boundary between accretion (i.e., growth of the target) and erosion.

velocity regime where impacts result in the erosion and dispersal of the target. In developing these scaling relations, simulations use targets and impactors of similar size and are conducted with $v_{\rm imp} \gtrsim 4v_{\rm esc}$ (e.g., Love & Ahrens 1996; Benz & Asphaug 1999). In general, the target mass is diminished by the collision. Extrapolation of these scaling relations to late-stage collisions predicts that only a few percent of the target is dispersed (ACL99). In the absence of direct modeling of the low-velocity regime ($v_{\rm imp} \simeq 1v_{\rm esc}$–$2v_{\rm esc}$), this has been inferred to mean that accretion is efficient. However, we now show that the lack of target disruption does not necessarily coincide with the effective merging of the impactor and target.

Perhaps most directly relevant to terrestrial planet formation is the work of Benz et al. (1988). They performed SPH impact simulations between differentiated planetary embryos with masses ~0.10 $M_\oplus$ to identify the type of collision needed to strip Mercury of a primordial mantle and test the efficacy of a collisional origin for its high density and iron content. Their simulations used an impactor-to-target mass ratio of about $M_i : M_t = 1 : 6$ and impact velocities in the range $v_{\rm imp} \approx 2.5v_{\rm esc}$–$8v_{\rm esc}$. All of their collisions resulted in net mass erosion of the target. Together, these previous works suggest that for collisions between planetary embryos, the dynamical transition between accretion (i.e., growth of the target) and erosion (i.e., net mass loss by the target) is at least as low as $v_{\rm imp} \lesssim 2.5v_{\rm esc}$–$4v_{\rm esc}$.

2.3. *Late-Stage Accretion Dynamics*

Modeling of stage 2 predicts that the late stage begins with tens to hundreds of lunar- to Mars-sized planetary embryos in the terrestrial region. Gravitational scattering between these embryos stir up their relative velocities to a value comparable to the escape velocity of the largest bodies (i.e., $v_\infty \approx v_{\rm esc}$ or $v_{\rm imp} \approx 1.4v_{\rm esc}$; see, e.g., Ward 1993). In the late-stage accretion simulations of ACL99, the self-stirring of embryos alone resulted in impact velocities in the range $v_{\rm imp}/v_{\rm esc} = 1.0$–$6.0$ with most in the range $v_{\rm imp}/v_{\rm esc} = 1.0$–$2.0$. Additional perturbations from Jupiter and Saturn tend to increase relative velocities by 50%–100% over the self-stirring values (e.g., Levison & Agnor 2003), whereas dynamical friction with a planetesimal swarm and/or tidal interactions with a remnant gas disk may reduce encounter velocities somewhat (Agnor & Ward 2002; Kominami & Ida 2002). Thus, it appears that collisions common to late-stage accretion are likely to span the range from efficient accretion ($v_{\rm imp} \approx v_{\rm esc}$) to catastrophic disruption and erosion of the target.

3. MODELING EMBRYO COLLISIONS

We use SPH to simulate collisions between two 0.10 $M_\oplus$ planetary embryos, sampling the impact dynamics expected to be common in the late stage. There is a wealth of literature on the SPH method (see, e.g., the review by Monaghan 1992), and it is widely used to model collisions of condensed solar system materials (e.g., Benz et al. 1989; Love & Ahrens 1996; Benz & Asphaug 1999; Asphaug et al. 1998). Our particular model is a descendant of the code used in Benz et al. (1986) and includes self-gravity but neglects internal strength as is appropriate for the large, gravity-dominated objects considered here. We use the Tillotson equation of state (see Appendix I of Melosh 1989) to construct equilibrated, differentiated planetary embryos of roughly terrestrial composition consisting of 30% iron and 70% basalt by mass.

Impact velocities range from $v_{\rm imp}/v_{\rm esc} = 1.0$ to 3.0 with spacing of 0.1 in the $v_{\rm imp}/v_{\rm esc} = 1.0$–$1.5$ range and spacings of 0.25 at higher impact velocities. Simulations were performed with impact angles of $\xi = 0°$, 30°, 45°, and 60°. This divides the range of impact orientations into quartiles (i.e., 25% of collisions will have $\xi < 30°$, …, etc.). Each simulation used about 20,000 SPH particles and was performed in the center of mass frame. The embryos were not initially rotating. Each simulation was run for 20 hr of model time. In most cases, the general morphology of the result was determined within a few hours of the initial impact. Energy and angular momentum errors are conserved to $\sim\mathcal{O}(10^{-3})$ or better.

4. RESULTS

After each collision, we use a friends-of-friends algorithm to identify contiguous clumps of SPH particles. Then we use an iterative procedure to find clumps that are gravitationally bound. After assigning individual SPH particles into bound or escaping aggregates, it is easy to examine the mass distribution and material composition of the collision outcome. We use this method to determine the mass of the largest gravitationally bound aggregate (M_1) and the largest aggregate in the escaping material (M_2). In this treatment, M_1 includes material falling back to the main clump as well as material bound in orbit around it (e.g., in a protosatellite disk).

4.1. *Collision Outcomes*

The mass of the largest bound aggregate scaled by the target mass (M_1/M_t) is shown in Figure 1 as a function of the impact velocity. For accretion to occur, the largest aggregate must be more massive than the original target (i.e., $M_1 > M_t$). The boundary between accretion (growth) and erosion (mass loss) of the target is indicated by a horizontal dashed line with $M_1/M_t = 1$. The mass escaping the largest aggregate is simply $M_{\rm esc} = M_i + M_t - M_1$ and easily identified from Figure 1. In Figure 2, the fraction of the escaping mass contained in the largest aggregate ($M_2/M_{\rm esc}$) is shown as a function of the impact velocity. Together Figures 1 and 2 illustrate that the general

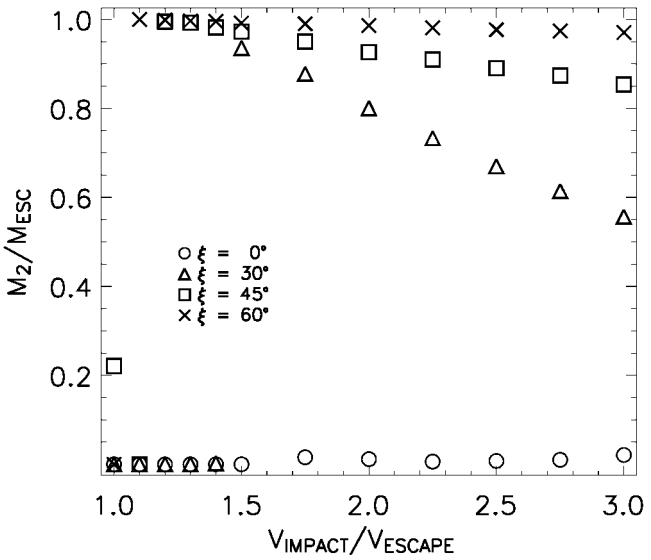

FIG. 2.—Fraction of escaping mass contained in the largest escaping aggregate (M_2) shown as a function of the impact velocity.

morphology of these collision outcomes is fairly simple and consists of one or two large aggregates and a spray of ejecta. The outcome is strongly dependent on impact angle.

For head-on collisions ($\xi = 0°$, shown with the open circles in Figs. 1 and 2), the outcomes consist of a single large aggregate and a spray of ejecta. At low impact velocities (i.e., $v_{\rm imp}/v_{\rm esc} < 1.5$), the two embryos effectively merge into a single object with minimal mass escaping the collision. At higher velocities, merging is less efficient with the mass of the largest aggregate decreasing linearly from $M_1/M_t = 1.85$ to 0.90 as $v_{\rm imp}/v_{\rm esc} = 1.5 \rightarrow 3.0$. In all these collisions, the escaping material consists predominantly of mantle particles. Consequently, at high impact velocity M_1 is iron-enriched, with the iron mass fraction slightly exceeding 0.5 for the $\xi = 0°$, $v_{\rm imp}/v_{\rm esc} = 3.0$ collision. This material fractionation result is similar to that of Benz et al. (1988). The mass of the largest escaping aggregate is small [$M_2/M_t \sim \mathcal{O}(10^{-2})$] for head-on collisions and never contains a sizable fraction of the escaping material (see Fig. 2).

Off-center collisions are different: typically, the two embryos collide and graze past each other. The impact, cratering, and rebound result in the conversion of some translational kinetic energy into rotational kinetic and internal energy. If the impact velocity is low enough, this renders the two objects gravitationally bound; they then suffer a second collision (with $v_{\rm imp}/v_{\rm esc} < 1.0$) that acts effectively as an inelastic merger with minimal mass escaping from M_1. This multiple-collision phenomenon has been observed before in low-velocity (i.e., $v_{\rm imp}/v_{\rm esc} \simeq 1.0$) Moon-forming impact simulations (e.g., Cameron 2001).

For faster $\xi = 45°$ and 60° collisions (shown in Figs. 1 and 2 with the open squares and crosses, respectively) with $v_{\rm imp}/v_{\rm esc} > 1.1$, the two colliders "bounce" inelastically and escape to infinity largely intact. Even for the highest impact velocities studied, the largest remnant is only slightly eroded by the collision ($M_1/M_t = 0.92$ and 0.97 for $v_{\rm imp}/v_{\rm esc} = 3.0$ collisions with $\xi = 45°$ and 60°, respectively). Figure 2 indicates that most of the mass escaping leaves in a single aggregate rather than as a shower of smaller particles.

For impacts with $\xi = 30°$ (shown in Figs. 1 and 2 with the open triangles), the transition between accretion and inelastic rebound occurs for $v_{\rm imp}/v_{\rm esc} > 1.4$. At these velocities, M_1 and M_2 suffer a greater level of erosion than for larger impact angles. The mass of two largest aggregates decreases linearly from $M_{1,2}/M_t = 0.96$ to 0.70 as the impact velocity increases from $v_{\rm imp}/v_{\rm esc} = 1.5$ to 3.0. Again, with the exception of the two largest aggregates, the remaining clumps in the escaping material are individually 2 orders of magnitude less massive than the initial embryos and consist almost exclusively of material from their mantles. Such collisions will tend to increase the iron fraction of surviving embryos while repopulating the planetesimal swarm with mantle material.

In some of the glancing collisions, the impact angular momentum exceeds that of a sphere of equivalent mass $M_t + M_i$ rotating with orbital speed at the surface. We find that the angular momentum of such collisions is processed in one of two ways: If the two objects are gravitationally bound after the initial impact, they subsequently merge and the system's angular momentum excess is spun out into a circumplanetary disk consisting primarily of mantle material (e.g., Canup & Asphaug 2003). On the other hand, if the impactor bounces and does not accrete, then the embryos are spun up slightly and much of the encounter angular momentum is carried off almost as though no collision had occurred.

It is curious that the results presented here are similar to those obtained by Leinhardt et al. (2000) and Benz (2000) in studies of low-speed collisions between small asteroidal rubble piles—a very different size, velocity, and mechanical regime. Gravitational interactions may thus dominate the collisional outcome in both regimes. Our ongoing efforts in both regimes seek to determine whether a unified scaling relation applies for collisional outcomes spanning a large mass and velocity range relevant to accretion.

4.2. *Relative Frequency of Outcomes*

We estimate the relative frequency of accretionary outcomes during planet formation by integrating over impact orientation and velocity distributions. We assume impact orientations are isotropic (Shoemaker 1962) and that encounter velocity distribution is well described by a Gaussian (as indicated by the *N*-body simulations of Ida & Makino 1992), where v_∞^* is the rms value. Furthermore, we assume that our simulation results with $\xi = 0°$ are representative of the quartile of collisions that occur with impact angles in the range $\xi = 0°$–30° and that our $\xi = 30°$ results are representative of all collisions with $\xi = 30°$–45°, …, etc. By using the lowest impact angle as representative of each bin, we overestimate the fraction of accretionary collisions.

From Figure 1, we identify the transition between accretionary and erosional collisions (i.e., $M_1 = M_t$) as occurring for $v_{\rm imp}/v_{\rm esc} > 2.8$, 1.4, 1.1, and 1.1 for impact angles of $\xi = 0°$, 30°, 45°, and 60°, respectively. We then integrate over the velocity distribution to estimate the fraction of collisions during planet formation that result in net growth of the target embryo as a function of the assumed rms encounter velocity (v_∞^*). For $v_\infty^* = v_{\rm esc}$, which is appropriate for a self-stirring distribution of embryos (e.g., Ward 1993), less than 55% of collisions result in accretion. Perturbations from Jupiter and Saturn might tend to increase encounter velocities between embryos near 1 AU to $v_\infty^* \simeq 1.5 v_{\rm esc}$. In this case, less than 40% of collisions result in accretion. Alternatively, if velocity damping (via dynamical friction and/or tidal interaction with a gas disk) reduces encounter velocities to $v_\infty^* \leq 0.5 v_{\rm esc}$, then the upper limit on the fraction of accretionary collisions increases to greater than

80%. In addition, the nonaccretionary collisions consist primarily of inelastic bouncing events with minimal erosion of the colliders but with dramatic geophysical consequences reported by Asphaug et al. (2003) and E. Asphaug et al. (2004, in preparation).

5. SIGNIFICANCE OF NONACCRETIONARY COLLISIONS

We have modeled collisions between identical 0.10 $M_{\oplus}$ differentiated planetary embryos with collision dynamics common to the late stage of terrestrial planet formation. The general morphology of the collision remnants consists of one or two large aggregates of mass comparable to the initial embryos along with a spray of much smaller ejecta. At low impact velocities ($v_{\rm imp}/v_{\rm esc} < 1.5$) and for more direct collisions (i.e., impact angles $\xi \leq 30°$), the impacts are largely accretionary, resulting in a single larger embryo and less than 10% of the mass escaping in much smaller clumps of ejecta. Inelastic bouncing between embryos with slight erosion followed by escape to infinity is a common outcome. This occurs for glancing collisions at low impact velocities (i.e., $v_{\rm imp}/v_{\rm esc} > 1.1$ and $\xi \geq 45°$) and more direct collisions at moderate impact velocity ($v_{\rm imp}/v_{\rm esc} > 1.4$ with $\xi \geq 30°$).

For dynamical environments typical of late-stage accretion models (i.e., $v_{\infty}^{*} \sim 1v_{\rm esc}$–$1.5v_{\rm esc}$; Chambers & Wetherill 1998; ACL99; Chambers 2001; Levison & Agnor 2003), we estimate that more than half of all collisions between like-sized planetary embryos do *not* result in accumulation into a larger embryo. While our initial results are limited to a single mass ratio, they suggest that nonaccretionary collisions are the norm during the end of terrestrial planet formation.

The collisional and dynamical accretion of planets are coupled. For example, the reduced accretion efficiency demonstrated above appears to lengthen the timescale of planet formation by a factor of 2 or more, relative to perfect mergers. The production of significant erosional debris, however, might alter the dynamical environment in ways that remain largely unexplored—for instance, damping the system to lower relative velocities. Detailed work in progress relates to this phenomenon of nonaccretionary collisions: its effects on the dynamics of planet growth, its geophysical processing and fractionation of material, as well as its predictions and implications for terrestrial planet diversity.

REFERENCES

Agnor, C. B., Canup, R. M., & Levison, H. F. 1999, Icarus, 142, 219 (ACL99)
Agnor, C. B., & Ward, W. R. 2002, ApJ, 567, 579
Asphaug, E., Agnor, C., Williams, Q., Petit, J., & Rivkin, A. 2003, AGU Fall Meeting, Abstr. P51F-04
Asphaug, E., Ostro, S. J., Hudson, R. S., Scheeres, D. J., & Benz, W. 1998, Nature, 393, 437
Benz, W. 2000, Space Sci. Rev., 92, 279
Benz, W., & Asphaug, E. 1999, Icarus, 142, 5
Benz, W., Cameron, A. G. W., & Melosh, H. J. 1989, Icarus, 81, 113
Benz, W., Slattery, W. L., & Cameron, A. G. W. 1986, Icarus, 66, 515
———. 1988, Icarus, 74, 516
Cameron, A. G. W. 2001, Meteoritics Planet. Sci., 36, 9
Canup, R. M. 2004, Icarus, 168, 433
Canup, R. M., & Agnor C. 2000, in Origin of the Earth and Moon, ed. R. M. Canup & K. Righter (Tucson: Univ. Arizona Press), 113
Canup, R. M., & Asphaug, E. 2001, Nature, 412, 708
———. 2003, Lunar Planet. Sci. Conf., 34, 1984
Chambers, J. E. 2001, Icarus, 152, 205
Chambers, J. E., & Wetherill, G. W. 1998, Icarus, 136, 304
Holsapple, K., Giblin, I., Housen, K., Nakamura, A., & Ryan, E. 2002, in Asteroids III, ed. W. F. Bottke, A. Cellino, P. Paolicchi, & R. P. Binzel (Tucson: Univ. Arizona Press), 443
Ida, S., & Makino, J. 1992, Icarus, 96, 107
Keil, K. 2000, Planet. Space Sci., 48, 887
Kokubo, E., & Ida, S. 1998, Icarus, 131, 171
Kominami, J., & Ida, S. 2002, Icarus, 157, 43
Leinhardt, Z. M., Richardson, D. C., & Quinn, T. 2000, Icarus, 146, 133
Levison, H. F., & Agnor, C. B. 2003, AJ, 125, 2692
Lissauer, J. J., Dones, L., & Ohtsuki, K. 2000, in Origin of the Earth and Moon, ed. R. M. Canup & K. Righter (Tucson: Univ. Arizona Press), 101
Lissauer, J. J., & Stewart, G. R. 1993, in Protostars and Planets III, ed. E. H. Levy & J. I. Lunine (Tucson: Univ. Arizona Press), 1061
Love, S. G., & Ahrens, T. J. 1996, Icarus, 124, 141
Melosh, H. J. 1989, Impact Cratering: A Geologic Process (New York: Oxford Univ. Press)
Monaghan, J. J. 1992, ARA&A, 30, 543
Shoemaker, E. M. 1962, in Physics and Astronomy of the Moon, ed. Z. Kopal (New York: Academic), 283
Ward, W. R. 1993, Icarus, 106, 274
Weidenschilling, S. J., Spaute, D., Davis, D. R., Marzari, F., & Ohtsuki, K. 1997, Icarus, 128, 429
Wetherill, G. W. 1990, Annu. Rev. Earth Planet. Sci., 18, 205
Wetherill, G. W., & Stewart, G. R. 1993, Icarus, 106, 190
Zhang, Y. 2002, Earth Sci. Rev., 59, 235